Journal of Biomechanics 84 (2019) 197–203

Contents lists available at ScienceDirect

Journal of Biomechanics

journal homepage: www.elsevier.com/locate/jbiomech
www.JBiomech.com

An *in vitro* experimental study on the relationship between pulsatile tinnitus and the dehiscence/thinness of sigmoid sinus cortical plate ☆

Shan Tian [a,b], Xingyu Fan [c], Yawei Wang [a,b], Zhaohui Liu [d,*], Lizhen Wang [a,b,*,1]

[a] *Key Laboratory for Biomechanics and Mechanobiology of Ministry of Education, School of Biological Science and Medical Engineering, Beihang University, Beijing 100083, China*
[b] *Beijing Advanced Innovation Center for Biomedical Engineering, Beihang University, Beijing 100083, China*
[c] *College of Bioengineering, Chongqing University, Chongqing 400044, China*
[d] *Department of Radiology, Beijing Tongren Hospital, Capital Medical University, Beijing 100730, China*

ARTICLE INFO

Article history:
Accepted 31 December 2018

Keywords:
Pulsatile tinnitus
Sigmoid sinus cortical plate
Venous sound
In vitro experiment
Dehiscence

ABSTRACT

Pulsatile tinnitus (PT), characterized as pulse-synchronous, is generally objective. Sigmoid sinus (SS) venous sound is widely suggested to be a possible sound source of PT. The dehiscence and thinness of SS cortical plate (CP) was commonly reported as PT pathology in previous studies, but lack quantitative or biomechanical analysis. In this study, it was aimed to quantify the relationship between venous sound and CP dehiscence/thinness using *in vitro* experiment. The *in vitro* models of SS and CP were established based on 3D-printing, with the developed pulsatile venous flow in the SS model. The generated sound signal and the vibration response at the dehiscent/thinned area were analyzed. The sound signal generated in the normal-sized dehiscence model was pulse-synchronous within 100-–400 Hz, which had similar acoustic characteristics as the clinical PT sounds. It was concluded that the pulsatile venous sound is produced at TS-SS junction in case of CP dehiscence. The CP, even a thinned one can effectively diminish the venous sound and sound-generating pulsatile vibration at TS-SS junction. The CP dehiscence would induce pulse-synchronous and high pressure venous sound, as well as pulse-synchronous vibration above 20 Hz, regardless of the dehiscence size. On the contrary, the CP thinness would not induce obvious venous sound or pulsatile vibration above 20 Hz.

1. Introduction

Pulsatile tinnitus (PT) is a tinnitus symptom characterized by the rhythm synchronized with the patient's heartbeat (McFerran and Phillips, 2007). Totally, more than one out of ten people are affected by tinnitus, while 4% of them are of PT (Stouffer and Tyler, 1990). PT is generally caused by objective somatosounds, especially the vascular sounds, and can be perceived by another person or sound-detection instrument (Kim et al., 2016; Sismanis, 2011; Song et al., 2016). Eisenman and Xue et al. suggested that the PT sounds might be produced by the venous sound originating from sigmoid sinus (SS), the closest vessel to the tympanic cavity (Eisenman, 2011; Xue et al., 2012). Previous numerical studies conducted by our group suggest that sound originating from the TS-SS junction is inaudible with normal cortical plate (CP) (Tian et al., 2017). However, some anomalies related to transverse sinus (TS) and SS (e.g., TS stenosis, SS diverticulum and CP dehiscence) were clinically hypothesized to amplify the SS venous sound, leading to the perception of PT (Boddu et al., 2016; Liu et al., 2013; Mundada et al., 2015).

It was assumed that the SS venous sound induced PT through air pathways of the temporal bone air cells (Liu et al., 2015; Tian et al., 2017). Overlying the lateral SS, the CP is clinically assumed to be a "soundproof wall", since it is the only hard tissue on the pathway of venous sound between the SS and the tympanic cavity (Zhao et al., 2016). The deficiencies in CP, including dehiscence and thinness, were commonly reported as PT pathologies (Eisenman, 2011; Geng et al., 2015; Liu et al., 2015; Raghavan et al., 2016; Tian et al., 2017; Xue et al., 2012), since they are common among PT patients, but are rare among non-tinnitus people (Krishnan

☆ This paper was not presented at any meetings and has not been accepted for presentation at a future meeting.

* Corresponding authors at: Department of Radiology, Beijing Tongren Hospital, Capital Medical University, 1# Dongjiaominxiang, Dongcheng district, Beijing 100730, China (Zhaohui Liu). Key Laboratory for Biomechanics and Mechanobiology of Ministry of Education, School of Biological Science and Medical Engineering, Beihang University, 37# Xueyuan Road, Haidian District, Beijing 100083, China (Lizhen Wang).

E-mail addresses: lzhtrhos@163.com (Z. Liu), lizhenwang@buaa.edu.cn (L. Wang).

[1] Secondary institution: Beijing Advanced Innovation Center for Biomedical Engineering, Beihang University, 37# Xueyuan Road, Haidian District, Beijing 100083, China.

https://doi.org/10.1016/j.jbiomech.2018.12.049
0021-9290/

et al., 2006; Schoeff et al., 2014). The CP dehiscence causes "air on sinus sign" that exposes the SS vessel to the air cells of temporal bone, resulting in the decline of soundproof effect (Geng et al., 2015). It was clinically hypothesized that the CP dehiscence could amplify the vibration response of exposed SS tissue, and thus induced audible sound signals (Eisenman, 2011; Liu et al., 2015; Raghavan et al., 2016).

Recently, the CP resurfacing surgery is a common treatment for the PT patients with CP dehiscence, and has a high cure rate up to 90% (Eisenman, 2011; Harvey et al., 2014). It can diminish the venous sound through fixing the CP deficiencies and skeletonizing the lateral SS surface (Eisenman, 2011; Raghavan et al., 2016; Santa Maria, 2013). However, it still remains uncertain whether it is necessary for the relatively small-sized dehiscence or thinness (without dehiscence) patients to be treated with the CP resurfacing surgery (Krishnan et al., 2006). Therefore, it is important to quantify the relationship between the venous sound and CP dehiscence size, and that between the venous sound and CP thickness. Besides, the mechanism and acoustic characteristics of venous sound have not been investigated in view of biomechanics in previous studies. This study aimed to simulate the venous sound signals using *in vitro* experiment, and further quantify the relationship between the venous sound and CP dehiscence size, and that between the venous sound and CP thickness. Moreover, the acoustic characteristics of the venous sounds and the vibration responses of SS tissue in the cases with different CP dehiscence size and CP thickness were also analyzed.

2. Methods

2.1. Radiology data collection

All radiological procedures performed in this study involving human participants were in accordance with the ethical standards of the institutional and national research committee and with the 1964 Helsinki declaration and its later amendments or comparable ethical standards. Informed consent was obtained from all individual participants included in the study.

The CT data were collected on a 37 year-old female PT patient, who had the right persistent PT and the ipsilateral CP dehiscence at TS-SS junction, with the dehiscent area of about 25 mm^2. No other obvious malformations were found along TS-SS. The CP resurfacing surgery was performed on this patient and the PT symptom was cured after surgery. The CT images were obtained using a 64-slice multi-detector scanner (Philips Medical Systems), with the injection of iodinated nonionic contrast material to exhibit the lumen of TS-SS. The CT images had the spatial resolution of 0.3125 mm, matrix size of 512 × 512.

The MR data were collected on 11 PT patients. The MR images were obtained using GE 3.0 Tsigna scanner (General Electric Healthcare), with the in-plane resolution of 0.78 mm, temporal resolution of 40 ms, slice thickness of 4 mm and matrix size of 256 × 256. The MR acquisition type was 2D phase-contrast cine-MR, including magnitude and phase images. The images were post-processed on GE adw4.4 workstation (General Electric Healthcare), using the Report card software (Rediker). The transient flow velocity at mid-TS in a cardiac cycle was measured by integrating across manually drawn regions of interest that closely enclosed the vessel on the phase image. The average ± standard deviation of mean velocity was 26.1 ± 6.1 cm/s, and the velocity pulsation (the difference between the maximum and minimum velocity) was 6.3 ± 3.3 cm/s. The cross-section area at mid-TS of the 3D TS-SS lumen model was 42.2 mm^2, thus the simulated venous flow was developed using the sinusoidal flux, of which the median was 11 ml/s, and the codomain was 9.7 ml/s-12.3 ml/s (34.8–44.4 L/h).

2.2. In vitro models of TS-SS and CP

The 3D geometry models were developed based on CT data. The TS-SS lumen was manually masked and then reconstructed to 3D geometry model using Mimics 17.0 (Materialise Technologies). The inlet section of the TS-SS lumen was positioned at mid-TS, while the outlet section was positioned at the terminal of SS. There were no branches in this segment. The 3D model of TS-SS vessel wall (Fig. 1a) was extracted based on the lumen model using Geomagic Studio 12 (Geomagic), with 1 mm thickness. The model of CP (Fig. 1b) was extracted based on the outer surface of the TS-SS vessel model, with 1 mm CP thickness (Tian et al., 2017). The dehiscent\thinned areas of CP were made at the lateral TS-SS junction, where most CP deficiencies took place (Xue et al., 2012). The dehiscent area was made circular, with diameter of 3 mm, 6 mm and 9 mm respectively in the three dehiscence cases, because it was reported that the averaged transverse diameter of dehiscence among patients was 6 mm, and the dehiscence width was ranged between 2 and 9 mm (Dong et al., 2016; Raghavan et al., 2016). For the thinness CP cases, the thinned area was made circular, with 6 mm diameter, and CP thickness of 0.25 mm, 0.5 mm and

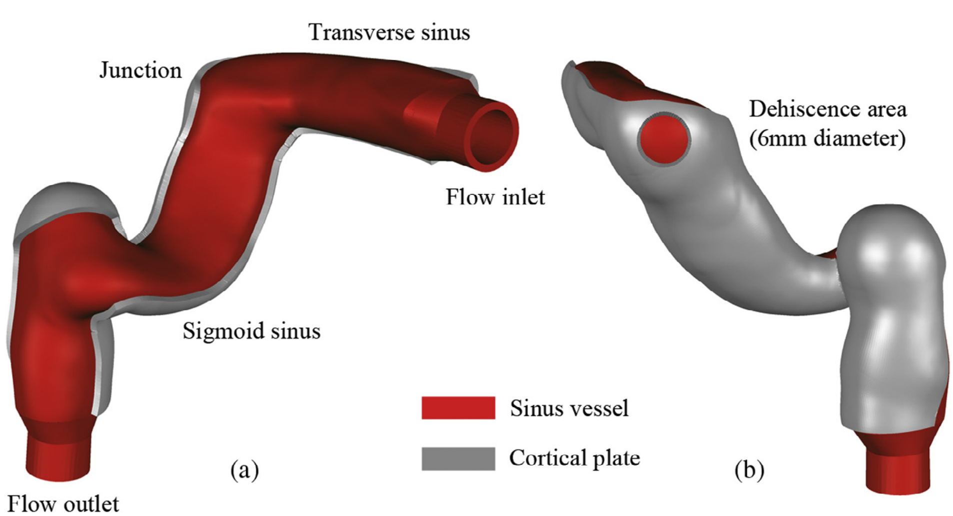

Fig. 1. The 3D models of: (a) TS-SS vessel; (b) CP plate with dehiscence.

0.75 mm respectively in the three thinness cases. The intactness case possessed intact 1 mm thickness CP overlying SS.

The *in vitro* models TS-SS and CP were 3D-printed using Form 2 (Formlabs). The TS-SS model was printed with the flexible resin material (FLFLGP02, Formlabs), while the CP models were printed with the solid resin material (FLGPWH04, Formlabs). After print, both the TS-SS vessel and CP models were soaked in isopropanol for 30 min to wash off the residual liquid resin, and then were solidified using ultraviolet ray with 405 nm length for 10 min.

2.3. In vitro experiment system

The *in vitro* experiment system consisted of a pulsation flow system, the *in vitro* models of TS-SS vessel and CP, and a sound recording chamber (Fig. 2a).

Construction of the simulated venous flow was performed using a self-designed pulsation system, which consisted of a peristaltic pump, a water capacitor, a water resistor, an electric piston and the control system. The piston performed the sine motion of 1.25 Hz (75 cardiac cycles per minute). The pulsation system was adjusted until the simulated venous flow obtained a sinusoidal flux with codomain of 34.8–44.4 L/h at the flowmeter. The static water was applied in the control case, while the simulated venous flow was applied in the other cases.

The microphone PZM-120 (Bjsound) with sensitivity up to −30 dB re 30 mV/Pa (1 V/Pa at 0 dB) was applied for sound recording. The *in vitro* TS-SS and CP model, as well as the sound recording chamber were positioned in a soundproof room. The dehiscent/thinned area was next to the chamber, while the microphone was placed inside the chamber, thus the dehiscent/thinned area was connected to the microphone through air pathway. Plasticine was used to keep the chamber totally sealed. The signals were recorded using the Audition 2017 CC software (Adobe), at a sampling rate of 48,000 Hz. The signals were then analyzed using Matlab 2017 (Mathworks).

The vibration displacement at the center of the dehiscent/thinned area was measured using the CD5-L25A laser displacement sensor (Optex-FA), with the repeat accuracy of 0.37 μm (Fig. 2b). The *in vitro* TS-SS and CP models were fixed right in front of the laser sensor, and the transient displacement was measured at the center of the dehiscent/thinned area, with the sampling frequency of 1250 Hz.

2.4. Signal analysis

The recorded signals were filtered using a Butterworth filter, with the cut-off frequencies of 100 and 1000 Hz, in order to filter out the noises induced by friction and wave. The signals within 100–1000 Hz were maintained and analyzed, since the PT sounds were reported normally low frequency (Kim et al., 2016; Song et al., 2016). The averaged peak values were obtained within 5 cardiac cycles (4 s) of the temporal analysis of sound signals (Kello et al., 2017). The short-time Fourier transform was performed for spectro-temporal analysis, with a Hann window of 128 samples and a hop size of 64 samples.

The measured vibration displacement was filtered using a Butterworth filter, with the cut-off frequency of 20 Hz, filtering out the response below 20 Hz. Therefore, the maintained vibration was 20–625 Hz and responsible for noise generation. The averaged peak amplitudes were obtained within 5 cardiac cycles (4 s) of the filtered temporal response. The short-time Fourier transform was also performed for spectro-temporal analysis, with a Hann window of 128 samples and a hop size of 64 samples.

3. Results

3.1. Temporal sound signals

The sound signals in 4 s time domain were illustrated in Fig. 3. No periodicity was shown in the signals of the control case and intactness case (a, h). Strong periodic structures were exhibited in the signals of all the dehiscence cases (b–d), with the same frequency (1.25 Hz) as the pulsation of simulated venous flow,

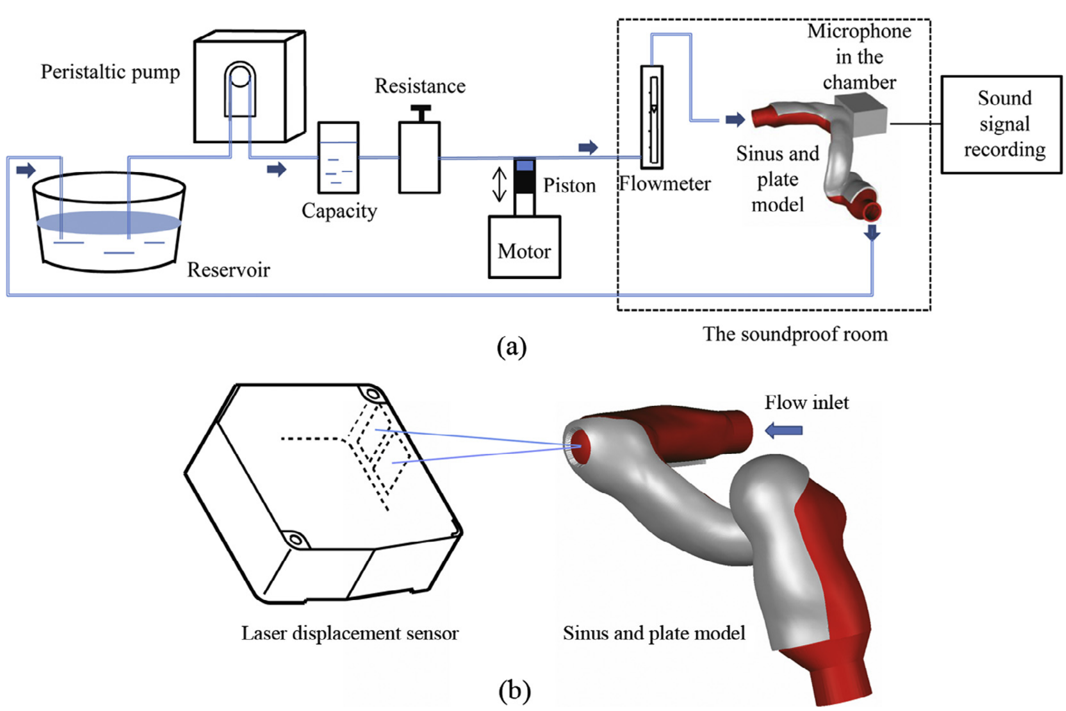

Fig. 2. The sketch of the in-vitro experiment system of: (a) simulation and recording of the venous sound; (b) displacement measurement at the center of dehiscent/thin area.

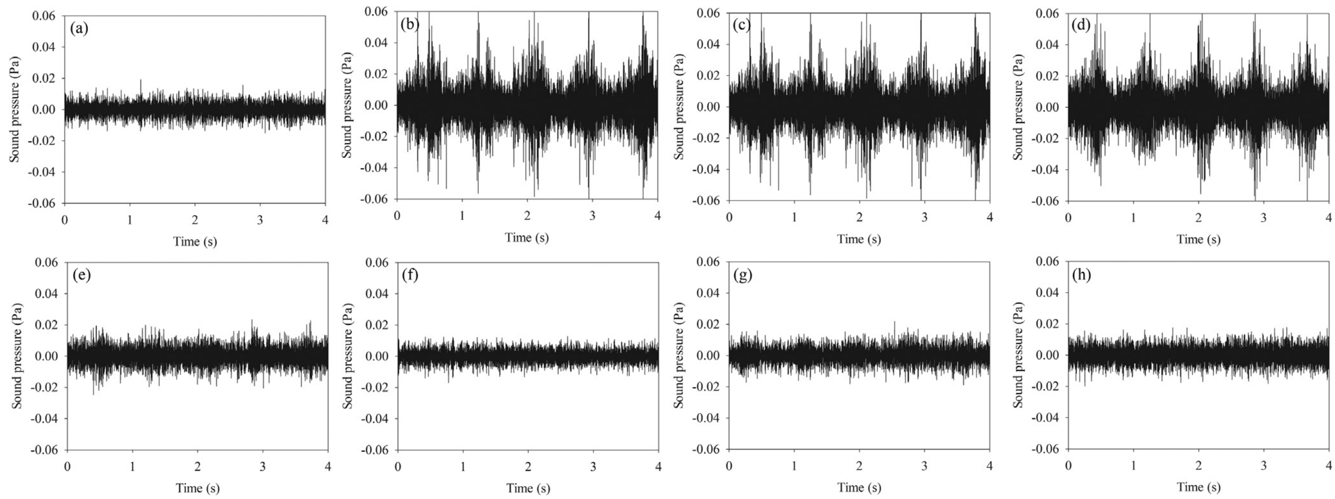

Fig. 3. The temporal results of the venous sound in: (a) Control case; (b) 3 mm dehiscence; (c) 6 mm dehiscence; (d) 9 mm dehiscence; (e) 0.25 mm thickness; (f) 0.5 mm thickness; (g) 0.75 mm thickness; (h) 1 mm intactness.

while much weaker or no periodic nature was shown in the signals of all the thinness cases (e–g).

The peak sound pressures were listed in Table 1. The peak sound pressures within 0.045–0.065 Pa were exhibited in the signals of all the dehiscence cases (b–d), while the peak pressures within 0.012–0.021 Pa were shown in the signals of all the non-dehiscence cases (a & e-h). The signals of all the non-dehiscence cases showed sound pressures close to the control signal, and were notably lower than those of all the dehiscence cases.

3.2. Temporal-spectral sound signals

The sound signals in time-frequency domain were illustrated in Fig. 4. No periodicity was shown in the signals of the control, intactness and 0.5 mm thickness cases (a, h, f). Strong pulse-synchronous structures within 200–1000 Hz were exhibited in the signal of the 3 mm dehiscence case (b), while those within 100–400 Hz were shown in the 6 mm and 9 mm dehiscence cases (c, d). Weak pulse-synchronous structures within 200–700 Hz were shown in the 0.25 mm and 0.75 mm thickness cases (e, g).

3.3. Temporal vibration responses

The filtered temporal vibration displacements (20–625 Hz) at the center of the dehiscent/thinned areas were illustrated in Fig. 5. No notable vibration response was exhibited in the control case (a), while the other cases showed vibration responses. The peak vibration amplitudes (20–625 Hz) were listed in Table 1. The control case showed peak amplitude of 2.898 μm (a). All the dehiscence cases exhibited peak amplitudes above 4.4 μm (b–d), while all the non-dehiscent cases showed peak amplitudes in the range of 2.3–3.9 μm (e–h). The vibration amplitudes in the dehiscence cases were higher than those in the thinness cases.

3.4. Temporal-spectral vibration responses

The filtered vibration displacements (20–625 Hz) in time–frequency domain were illustrated in Fig. 6. As the pulsatile vibration was mainly limited to 20–150 Hz, Fig. 7 was added to zoom in on this frequency domain. Obvious periodicity between 20 and 150 Hz was shown in all the dehiscence cases (b–d). No obvious periodicity was shown in the control and all thinness cases (a, e–h).

Table 1
The peak sound pressures of the filtered signals and peak amplitudes of the filtered vibration responses (20–625 Hz).

Case		Peak sound pressure (Pa)	Peak vibration amplitude (μm)
a	Control	0.0146	2.898
b	3 mm dehiscence	0.0455	8.909
c	6 mm dehiscence	0.063	4.442
d	9 mm dehiscence	0.0602	7.789
e	0.25 mm thickness	0.0207	2.989
f	0.5 mm thickness	0.0129	3.845
g	0.75 mm thickness	0.017	3.449
h	1 mm Intactness	0.0173	2.368

4. Discussion

It is commonly suggested that the venous sound originating from SS is a possible sound source of PT (Eisenman, 2011; Geng et al., 2015; Xue et al., 2012). The venous sound might induce PT through the air pathway of temporal bone air cells (Liu et al., 2015; Tian et al., 2017). However, there is lack of acoustic analysis on the venous sound. Besides, the mechanism of venous sound generation has not been verified. In this study, we simulated the TS-SS venous flow using *in vitro* experiment, and recorded and analyzed the generated sound signals. The anatomical structures and mechanical properties of TS-SS vessel and CP were simulated, as well as the pulsatile venous flow inside the vessel. Specifically, the 3D geometry models of TS-SS vessel and CP were digitally reconstructed based on the CT data of a PT patient, who has the ipsilateral CP dehiscence at TS-SS junction, and no more malformation was found along TS-SS. Afterwards, the *in vitro* TS-SS vessel wall was 3D-printed using the flexible resin material, of which the Young's modulus was ∼3.6 MPa, close to the vein vessel wall (∼1.25 MPa (Lofink and Müller, 2013; Narracott et al., 2015)), and could withstand the pulsatile water pressure at the same time. The *in vitro* CP model was 3D-printed using the solid resin material, of which the Young's modulus was ∼3 GPa, close to the cortical bone (∼9 GPa (Pereira et al., 2018)), and was rigid enough to simulate the soundproof effect of CP. Moreover, the median and codomain of the simulated venous flux were set according to the average flow velocity at mid-TS of 11 PT patients.

The results obtained in this study are in accordance with the clinical findings. Firstly, the simulated venous sound in the 6 mm

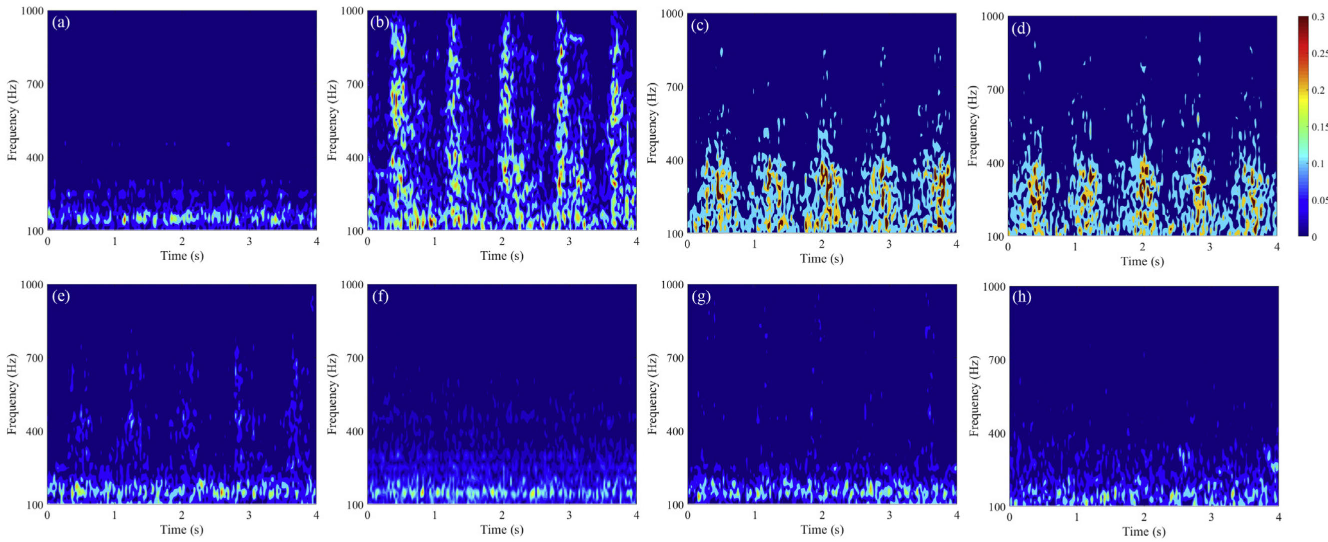

Fig. 4. The spectral-temporal results of the venous sound in: (a) Control case; (b) 3 mm dehiscence; (c) 6 mm dehiscence; (d) 9 mm dehiscence; (e) 0.25 mm thickness; (f) 0.5 mm thickness; (g) 0.75 mm thickness; (h) 1 mm intactness.

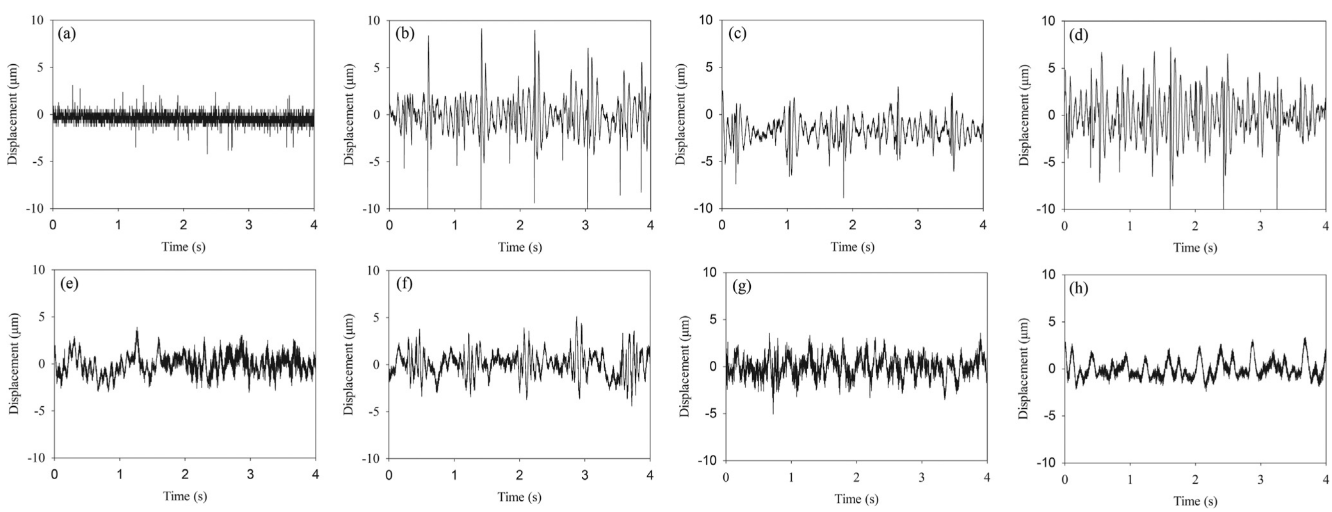

Fig. 5. The temporal vibration displacement (20–625 Hz) at the dehiscent\thinned center of: (a) Control case; (b) 3 mm dehiscence; (c) 6 mm dehiscence; (d) 9 mm dehiscence; (e) 0.25 mm thickness; (f) 0.5 mm thickness; (g) 0.75 mm thickness; (h) 1 mm intactness.

dehiscence case exhibited the similar temporal and spectral structures as the real PT sounds. The recorded sound signal in the 6 mm dehiscence case exhibited obvious pulse-synchronous structures within 100–400 Hz. Similarly, the PT sounds were always subjectively reported as pulse-synchronous and low pitch (lower than 600 Hz) (Li et al., 2014). Moreover, the PT sounds recorded on patients were significantly stronger than that on non-tinnitus people in 125–500 Hz octave bands (Kim et al., 2016). Therefore, it was verified that the simulated venous sound in this study was valid and effective, and the SS venous flow could generate pulsatile venous sound. Moreover, the SS venous sound was a sound source of PT. Secondly, the recorded sound signal in the intactness case was aperiodic, with the peak sound pressure close to the background sound. It was indicated that the simulated venous sound in the intact CP case was inaudible, which was in accordance with the clinical findings that almost all the non-tinnitus people exhibited intact CP (Schoeff et al., 2014).

The CP was clinically hypothesized as a vital ‘‘venous sound blocker”, since it was the only hard tissue between the TS-SS and the tympanic cavity (Zhao et al., 2016). The dehiscence and thinness of CP were hypothesized to amplify the venous sound and induce PT (Eisenman, 2011; Liu et al., 2015; Raghavan et al., 2016). For CP dehiscence, it would induce an ‘‘air-on-sinus” sign: The sinus vessel directly contact the air cells of temporal bone, which might amplify the venous sound through increasing the vibration amplitude of exposed SS vessel. CP thinness was also common among PT patients, but its effect on amplifying the venous sound remained unknown (Krishnan et al., 2006). This study quantified the relationship between the venous sound and CP dehiscence size, and that between the venous sound and CP thickness.

High pressure and pulse-synchronous venous sounds were collected in all the dehiscence cases, regardless of the dehiscence size. On the contrary, all the non-dehiscence cases generated low pressure venous sounds, whose pressure was close to the background sound. Therefore, it was suggested that the CP dehiscence would directly induce pulsatile and high pressure venous sound, regardless of the dehiscence size, while the CP thinness would not induce obvious venous sound without any other causes. The hypothesis was verified that CP is an effective soundproof tissue. Even a

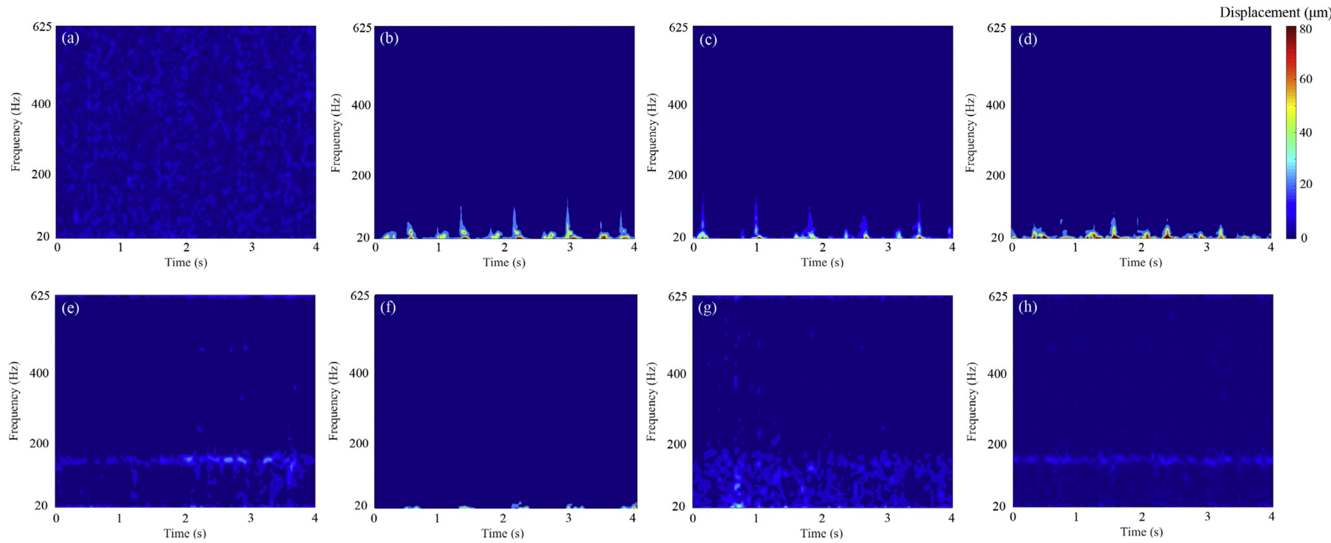

Fig. 6. The temporal-spectral vibration displacement (20–625 Hz) at the dehiscent\thinned center of: (a) Control case; (b) 3 mm dehiscence; (c) 6 mm dehiscence; (d) 9 mm dehiscence; (e) 0.25 mm thickness; (f) 0.5 mm thickness; (g) 0.75 mm thickness; (h) 1 mm intactness.

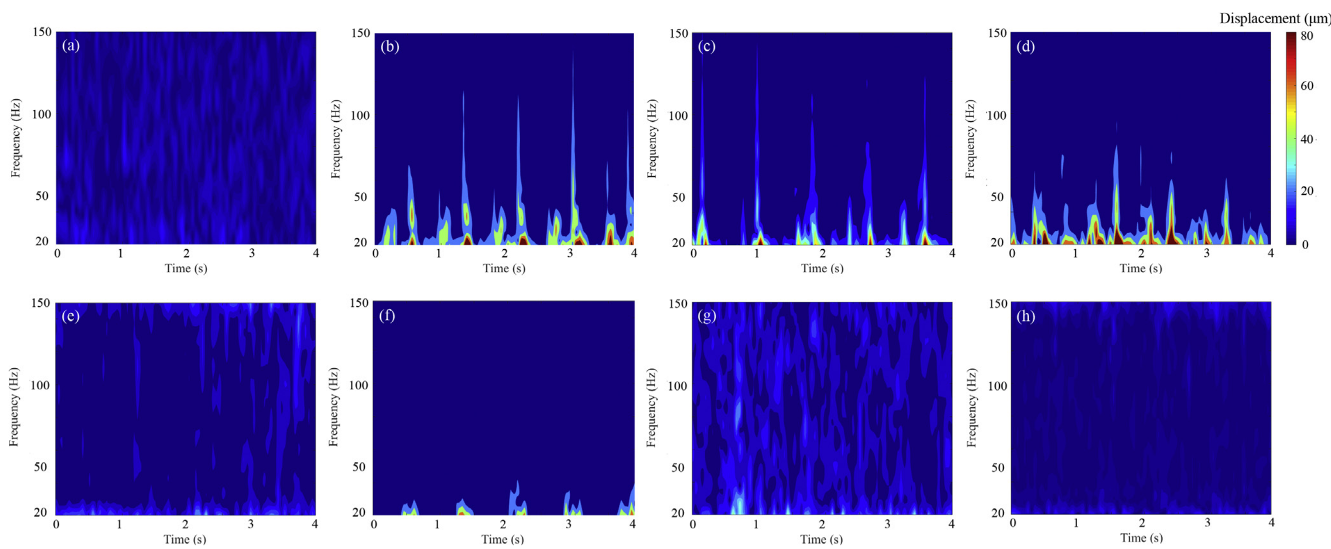

Fig. 7. The temporal-spectral vibration displacement (zooms in on 20–150 Hz) at the dehiscent\thinned center of: (a) Control case; (b) 3 mm dehiscence; (c) 6 mm dehiscence; (d) 9 mm dehiscence; (e) 0.25 mm thickness; (f) 0.5 mm thickness; (g) 0.75 mm thickness; (h) 1 mm intactness.

thinned CP can strongly diminish venous sound. For the PT patients with CP dehiscence, the dehiscence should be emphasized for its notable contribution amplifying venous sound. For the PT patients with thinned CP but without dehiscence, the other possible pathologies (e.g., vascular stenosis or extensive pneumatization of temporal bone air cells) might contributed primarily to the amplification of venous sound, and should be noticed.

In many previous studies, the vibration response of exposed SS tissue (Eisenman, 2011; Liu et al., 2015; Raghavan et al., 2016) was hypothesized as the origination of the SS venous sound. In this study, the vibration response at the dehiscent area was focused and investigated. The measured displacements were filtered, maintaining vibration above 20 Hz, which was directly responsible for noise generation. The results indicated that the vibration amplitudes (20–625 Hz) in the dehiscence cases were higher than those in the cases with thinned or intact CP. The dehiscence cases exhibited obvious pulsation in vibration within 20–150 Hz, which was not shown in the thinness and intactness cases. We concluded that even thinned CP notably diminished both the venous sound and sound-generating pulsatile vibration. Additionally, pulsatile sound between 100 and 1000 Hz and pulsatile vibration between 20 and 150 Hz were exhibited in case of CP dehiscence. This finding cannot conclude that PT was directly induced by the pulsatile vibration at the dehiscence area, since the venous sound had higher frequency than the pulsatile vibration. We can make some speculations for explanation: Firstly, besides the 20–150 Hz vibration, the flow field in TS-SS lumen could generate venous sound over 150 Hz, which might be diminished by the intact CP, while be leaked out with CP dehiscence. Secondly, the other parts of TS-SS besides the dehiscence area might generate venous sound over 150 Hz. Thirdly, the measurement of vibration over 150 Hz might be limited by the sensitivity of laser sensor. Although the mechanism remains uncertain, the noted pulsatile vibration above 20 Hz might make important contribute to the venous sound generation, and worth further investigation.

There are several limitations in this study. Firstly, the geometry models of TS-SS and CP, as well as the venous flow inlet were based on the CT data of one PT patient, limiting the scope of the results.

Secondly, the experiment is based on some assumptions. Only the venous sound originating from TS-SS junction was analyzed as a main sound source of PT. Moreover, the recorded venous sound was through air transmission, while the possible bone conduction was not included in this experiment. Thirdly, distilled water was used in the pulsation system instead of blood plasma, which might decrease the viscosity of fluid and affect the acoustic properties of venous sound. These limitations could be improved in the future study. Firstly, we could further address the properties of venous sound generated by various venous conditions, including the dominance, stenosis and diverticulum of TS-SS, preventing the limitation of a single geometry and flow pattern. Secondly, a more detailed *in vitro* model of temporal bone tissue might be helpful to analyze other possible sound sources and sound transmission pathways in the future. Thirdly, the glycerol solution could be used to obtain similar viscosity as blood plasma.

5. Conclusion

Through *in vitro* experiment, it is concluded: the pulsatile venous sound is produced at TS-SS junction in case of CP dehiscence. The CP, even a thinned one can effectively diminish the venous sound and sound-generating pulsatile vibration at TS-SS junction. The CP dehiscence would induce pulse-synchronous and high pressure venous sound, as well as pulse-synchronous vibration above 20 Hz, regardless of the dehiscence size. On the contrary, the CP thinness would not induce obvious venous sound or pulsatile vibration above 20 Hz.

6. Authors' contribution and claim

All authors claimed to have made substantial contributions to all of the following: (1) the conception and design of the study, or acquisition of data, or analysis and interpretation of data, (2) drafting the article or revising it critically for important intellectual content, (3) final approval of the version to be submitted. Each of the authors has read and concurs with the content in the manuscript.

All authors claim that the materials within this paper entitled "An *in vitro* experimental study on the relationship between pulsatile tinnitus and the dehiscence/thinness of sigmoid sinus cortical plate" has not been and will not be submitted for publication elsewhere except as an abstract.

7. Research ethics

All procedures performed in studies involving human participants were in accordance with the ethical standards of the institutional and national research committee and with the 1964 Helsinki declaration and its later amendments or comparable ethical standards. Informed consent was obtained from all individual participants included in the study.

Conflict of interest statement

This manuscript has been read and agreed by all authors without any commercial relationships which may lead to a conflict of interests.

Acknowledgement

This work was supported by grants (11421202, 11572029, and 81371545) from National Natural Science Foundation of China, grant (Z161100004916041) from Beijing Nova Program Interdisciplinary Studies Cooperative Projects, and grant (2015-3-016) from Beijing Health System High-level Health Technical Personnel Training Program.

Appendix A. Supplementary material

Supplementary data to this article can be found online at https://doi.org/10.1016/j.jbiomech.2018.12.049.

References

Boddu, S., Dinkin, M., Suurna, M., Hannsgen, K., Bui, X., Patsalides, A., 2016. Resolution of pulsatile tinnitus after venous sinus stenting in patients with idiopathic intracranial hypertension. Plos One 11, (10) e0164466.
Dong, C., Zhao, P., Liu, Z., Xu, W., Lv, H., Pang, S., Wang, Z., 2016. Association between the extent of sigmoid sinus dehiscence and an occurrence of pulsatile tinnitus: a retrospective imaging study. Clin. Radiol. 71 (9), 883–888.
Eisenman, D.J., 2011. Sinus wall reconstruction for sigmoid sinus diverticulum and dehiscence: a standardized surgical procedure for a range of radiographic findings. Otol. Neurotol. 32 (7), 1116–1119.
Geng, W., Liu, Z.H., Fan, Z.M., 2015. CT characteristics of dehiscent sigmoid plates presenting as pulsatile tinnitus: a study of 23 patients. Acta Radiol. 56 (11), 1404–1408.
Harvey, R.S., Hertzano, R., Kelman, S.E., Eisenman, D.J., 2014. Pulse-synchronous tinnitus and sigmoid sinus wall anomalies: descriptive epidemiology and the idiopathic intracranial hypertension patient population. Otol. Neurotol.: Off. Publ. Am. Otol. Soc., Am. Neurotol. Soc. Eur. Acad. Otol. Neurotol. 35 (1), 7–15.
Kello, C.T., Bella, S.D., MeDe, B., Balasubramaniam, R., 2017. Hierarchical temporal structure in music, speech and animal vocalizations: jazz is like a conversation, humpbacks sing like hermit thrushes. J. R. Soc. Interface 14 (135), 20170231.
Kim, S.H., An, G.S., Choi, I., Lee, K., Song, J.J., 2016. Pre-treatment objective diagnosis and post-treatment outcome evaluation in patients with vascular pulsatile tinnitus using transcanal recording and spectro-temporal analysis. Plos One 11, (6) e0157722.
Krishnan, A., Mattox, D.E., Fountain, A.J., Hudgins, P.A., 2006. CT arteriography and venography in pulsatile tinnitus: preliminary results. Am. J. Neuroradiol. 27 (8), 1635–1638.
Li, B.M., Cao, X.Y., Liu, X.F., Li, S., Wang, J., Liang, Y.P., Ge, A.L., Zhang, A., Feng, H.M., 2014. Interventionai diagnosis and treatment of vasculogeneic pulsatile tinnitus. J. Otol. 9 (1), 7–15.
Liu, W., Liu, Z., Zheng, N., Zhao, P., Dong, C., Wang, Z., 2015. Temporal bone pneumatization and pulsatile tinnitus caused by sigmoid sinus diverticulum and/or dehiscence. BioMed Res. Int. 2015, 970613.
Liu, Z., Chen, C.F., Wang, Z.C., Gong, S.S., Xian, J.F., Wang, Y.Z., Liang, X.H., Ma, X.B., Li, Y., 2013. Sigmoid sinus diverticulum and pulsatile tinnitus: analysis of CT scans from 15 cases. Acta Radiol. 54 (7), 812–816.
Lofink, P., Müller, W.H., 2013. Numerical modeling of fluid-structure interaction of blood in a vein by simulating conservation of mass and linear momentum with the finite element method in FEniCS. Pamm 13 (1), 209–210.
McFerran, D.J., Phillips, J.S., 2007. Tinnitus. J. Laryngol. Otol. 121 (3), 201–208.
Mundada, P., Singh, A., Lingam, R.K., 2015. CT arteriography and venography in the evaluation of Pulsatile tinnitus with normal otoscopic examination. Laryngoscope 125 (4), 979–984.
Narracott, A.J., Keijsers, J.J., Leguy, C., Huberts, W.W., De, F.F.V., Van, 2015. Fluid-structure interaction analysis of venous valve hemodynamics. CMBE2015), 29 June - 21 July 2015, France.
Pereira, B., Xavier, J., Pereira, F., Morais, J., 2018. Identification of transverse elastic properties of the diaphysis of cortical bone. IJMEM I (k), 27–32.
Raghavan, P., Serulle, Y., Gandhi, D., Morales, R., Quinn, K., Angster, K., Hertzano, R., Eisenman, D., 2016. Postoperative imaging findings following sigmoid sinus wall reconstruction for pulse synchronous tinnitus. Am. J. Neuroradiol. 37 (1), 136–142.
Santa Maria, P.L., 2013. Sigmoid sinus dehiscence resurfacing as treatment for pulsatile tinnitus. J. Laryngol. Otol. 127 (Suppl 2), S57–S59.
Schoeff, S., Nicholas, B., Mukherjee, S., Kesser, B.W., 2014. Imaging prevalence of sigmoid sinus dehiscence among patients with and without pulsatile tinnitus. Otolaryngol. Head Neck Surg. 150 (5), 841–846.
Sismanis, A., 2011. Pulsatile tinnitus: contemporary assessment and management. Curr. Opin. Otolaryngol. Head Neck Surgery 19 (5), 348–357.
Song, J.J., An, G.S., Choi, I., De, R.D., Kim, S.Y., Choi, H.S., Park, J.H., Choi, B.Y., Koo, J.W., Lee, K., 2016. Objectification and differential diagnosis of vascular pulsatile tinnitus by transcanal sound recording and spectrotemporal analysis: a preliminary study. Otol. Neurotol. 37 (6), 613–620.
Stouffer, J.L., Tyler, R.S., 1990. Characterization of tinnitus by tinnitus patients. J. Speech Hearing Disorders 55 (3), 439–453.
Tian, S., Wang, L., Yang, J., Mao, R., Liu, Z., Fan, Y., 2017. Sigmoid sinus cortical plate dehiscence induces pulsatile tinnitus through amplifying sigmoid sinus venous sound. J. Biomech. 52, 68–73.
Xue, J., Li, T., Sun, X., Liu, Y., 2012. Focal defect of mastoid bone shell in the region of the transverse-sigmoid junction: a new cause of pulsatile tinnitus. J. Laryngol. Otol. 126 (4), 409–413.
Zhao, P.F., Han, L., Cheng, D., Niu, Y.T., Xian, J.F., Wang, Z.C., 2016. CT evaluation of sigmoid plate dehiscence causing pulsatile tinnitus. Eur. Radiol. 26 (1), 9–14.